This is a peer-reviewed, accepted author manuscript of the following article: Zhao, S., Fan, Y., & Zhang, X. (2019). Influence of parameters on flame expansion in a high-speed flow: experimental and numerical study. *Proceedings of the Institution of Mechanical Engineers, Part A: Journal of Power and Energy* . https://doi.org/10.1177/0957650919896504

Influence of parameters on flame expansion in a high-speed flow: Experimental and numerical study

Zhao Shilong

Nanjing University of Aeronautics and Astronautics, 210016Nanjing, People's Republic of China;

E-mail: shilong.zhao@foxmail.com

Fan Yuxin*

Nanjing University of Aeronautics and Astronautics, 210016Nanjing, People's Republic of China;

E-mail: fanyuxin@nuaa.edu.cn

Zhang Xiaolei

School of Mechanical and Aerospace Engineering, Queen's University Belfast, BT9 5AH, UK;

E-mail: Xiaolei.zhang@qub.ac.uk

Abstract

Flameholder-stabilized flames are conventional also commonly used in propulsion and various power generation field to maintain combustion process. The characteristics of flame expansion was obtained with various blockage-ratios, which was observed to be highly sensitive to inlet conditions such as temperatures and velocities. Experiments and simulations combined methodology was performed, also the approach adopted on image processing was calculated automatically through a program written in MATLAB. It was found that the change of flame expansion angle indicated increasing fuel supply could contribute to the growth of flame expansion angle in lean premixed combustion. Besides, the influence of inlet velocity on flame expansion angle varies with different blockage ratios, i.e. under a small blockage ratio (BR=0.1), flame expansion angle declined with the increase of velocity;

however, under a larger blockage ratio (BR=0.2 or 0.3), flame expansion angle increased firstly and then decreased with the increasing velocity. Likewise, flame expansion angle increased firstly and then decreased with the increasing temperature under BR=0.2/0.3. In addition, flame expansion angle was almost the same for BR=0.2 and BR=0.3 at a higher temperature (900K), and both of which were bigger than BR=0.1. Overall, BR0.2 is the best for increasing flame expansion angle and reducing total pressure loss. The influence of velocity and temperature on flame expansion angle found from this research are vital for engineering practice and for developing a further image processing method to measure flame boundary.

Keywords

V-gutter; flame expansion angle; image processing; premixed flame; flame boundary; afterburner

1. Introduction

In modern power generation and propulsion devices, combustion typically took place under highly turbulent conditions. The turbulent flow conditions arose from high-speed turbulent inlet flow (free stream turbulence) as well as turbulence generated by the flame stabilization scheme. Flame holding devices such as V-gutter are commonly used in propulsion and various industrial systems to ignite and maintain the stable combustion process in a high-speed flow. An extensive amount of researches on flame holder has been performed over the past 70 years, making it one of the most commonly studied topics in turbulent combustion [1-2]. Most of the earlier studies on V-gutter focused on the flame stabilization mechanism, ignition and blow-off limits in steady combustion, and the conditions and mechanism of the occurrence of unsteady combustion.

*Corresponding Author: Prof. Fan Yuxin

Extensive studies have focused on the break-up and mixing of fuel in the air to increase the performance of combustion [3-7]. A numerical model of the fuel-air mixing process had been come up to identify key design parameters involved in fuel-air mixing and to characterize how mixing performance scales with the Reynolds number [8]. At the same time, the interaction of swirl flow with partial premixed and disk-stabilized flame was investigated [9]. Ignition and blow-off are directly affected by mixing of fuel and air [10]. Experimental study on lean ignition and blow-off indicated the change laws under various flow conditions and geometry parameters [11, 12]. In addition to flame propagation and stability issues, planar laser induced fluorescence technique and ICCD camera were used to obtain simultaneous imaging of hydroxyl and formaldehyde, as well as the flame spreading process [13-17]. Also, numerical simulation of flame propagation and stability had been done via large eddy simulation using global and skeletal reaction mechanisms [18-22]. Moreover, exhaust emissions and combustion efficiency are key indexes for combustion organization. Plenty of experiments had been conducted to investigate the effect of bluff body in steady and unsteady combustion [23-27]. Besides these studies on stabilizer, a number of experimental studies have been performed to investigate the effect of turbulence on premixed flames as summarised in the review papers of Driscoll [28], Clavin [29], Lipatnikov and Chommiak [30]. Based on the different flame geometries, they can be classified as the “Envelope” (Bunsen-type flames), “Oblique” (V-shaped flames), “Unattached” (low swirl or counterflow flames) categories and propagating flame kernels. Nevertheless, research on flame circumferential expansion angle of bluff-body is rare in the previous work. Indeed, the space of adjacent stabilizers is extremely important to circumferential flame spreading and axial distance of flame joint. It is essential for the flame front traveling through the entire burner cross section before it reaches the exit in an afterburner or a ramjet burner. The afterburner/ramjet burner is evenly distributed with stabilizers whose number depends on the

*Corresponding Author: Prof. Fan Yuxin

V-gutter width and the spacing of the adjacent struts. And also the flame stability and propagation performance varies with flow conditions.

To better understand the flame circumferential expansion after the flame anchored behind the stabilizer, experiments combined with simulations are necessary [31]. The influence of velocity, temperature and blockage ratio on flame expansion was investigated and stated the reason. Meanwhile, a new image processing method was implemented. The change of flame expansion angle was presented to be a reference for the selection and distribution of stabilizers in practical application.

2. Methodology

In this study, flame images was recorded using high speed camera and processed automatically through a program written in MATLAB. Numerical simulation was auxiliary method to analyse the change of flame expansion.

2.1 Experimental setup

Fig.1 showed the experimental set-up which consisted of air supply system, fuel supply system, preheating system, measurement system and burner with V-gutters. The facility simulated burner inlet conditions with various inlet temperatures (450-900K) and velocities (50-200m/s).

The air supply system consisted of two sets of Roots blowers whose maximum flow rate could reach 3kg/s and the highest air-supply pressure reach 0.17 MPa, two flow control valves, and two digital vortex shedding flowmeters with temperature-pressure compensation for control and measurement. The fuel supply system consisted of fuel pumps which could achieve 7 MPa fuel pressure, injectors, flow control valves, rotameters and digital metal tube flowmeters. To ensure the accuracy, the measured valves, rotameters and digital metal tube flowmeters were tested and calibrated before each experiment. The preheating system

*Corresponding Author: Prof. Fan Yuxin

contains combustor 1 and 2 that heat ambient air to hot gas, the mixing chamber, and the rectifier section. The measurement system involved several thermocouples that measured the temperature of preheating system outlet and burner inlet, flue gas analyser placed at rectifier section to examine the hot gas components, and a high-speed camera.

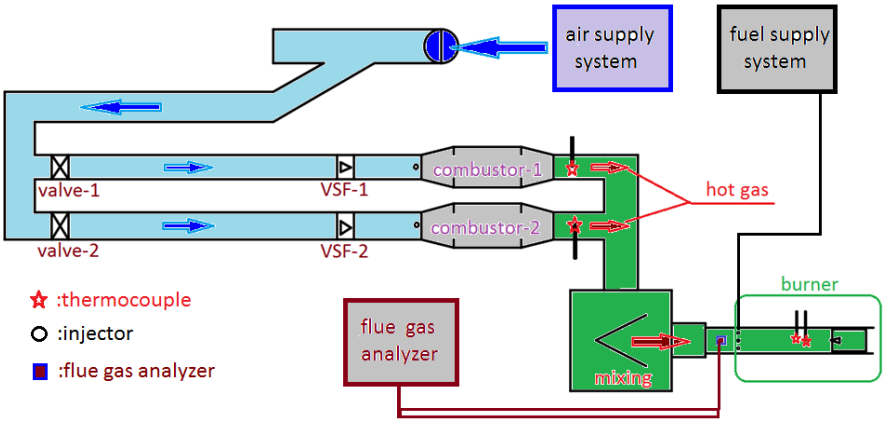

Fig.1 Structure of experimental system

The burner consisted of a cross-section with a horizontal length of 100mm and a vertical length of 150mm as well as sidewalls made of quartz windows, allowing full optical access to the flame shown in Fig.2. Three widths (W=15mm, 30mm, 45mm) of the V-gutter were designed to investigate the change of flame expansion at various flow conditions. Flame images were recorded in premixed combustion. To form evenly mixed fuel/air distribution, nine fuel injectors distributed averagely in the inlet cross section and were located 600mm upstream of the V-gutter, as well as injected Jet-A fuel across the main flow.

*Corresponding Author: Prof. Fan Yuxin

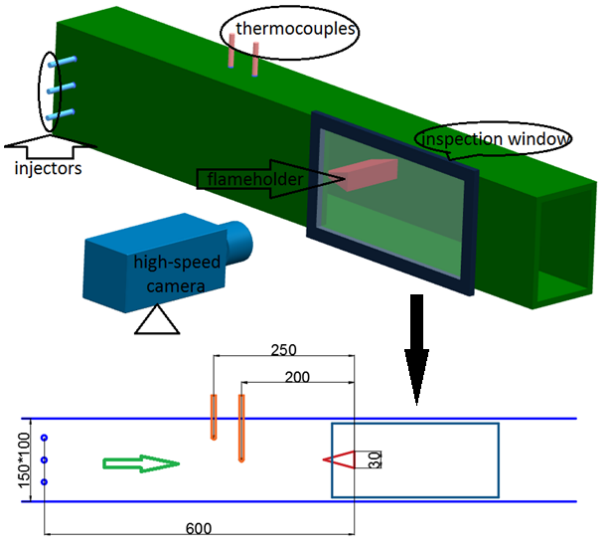

Fig.2 Enlarged burner (3D) of physical dimension (2D)

A high-speed camera (IDT, Y5 shown in Fig.2.(a)) used in this experiment surpassed high definition with a 4.0 megapixel sensor capable of 730 frames per second (fps) at full resolution, which was applied to record the time evolutions of flame expansion with reduced vertical resolution at a rate of 1000 fps.

2.2 Image processing

The flame expansion angle was calculated automatically through a program written in MATLAB. A new image processing method was developed including 7 steps as shown in Fig.3.

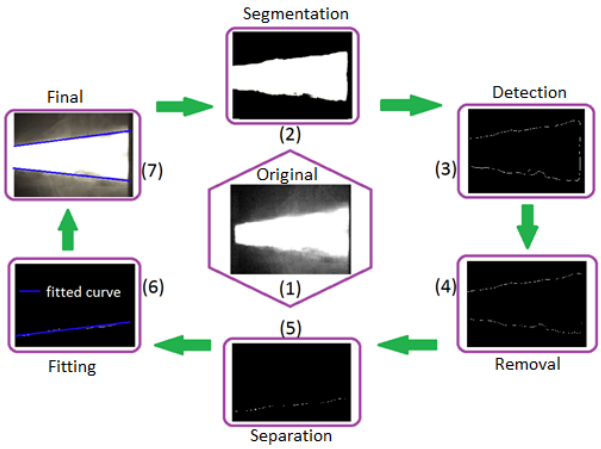

*Corresponding Author: Prof. Fan Yuxin

Fig.3 Images processing chart

The image in Step 1 showed one of the 100 original images taken by high-speed camera over a time interval for 1ms. During Step 2, the original images processed by the discretization method were divided into m rows and n columns, which constructed an $m \times n$ matrix whose numeric values depended on light intensity. Numeric values determined boundaries location of flame expansion. Firstly, the maximum gradients of numerical values in the column dimensions should be marked and analyzed. Secondly, comparisons were made with the lower and the higher numeric values shown in Fig.4, and the fit curve at different numerical values depict flame boundaries. Thirdly, segmentation was completed by numeric value range (>200). The final processing images Fig.3.(7) obtained under the given numeric value range above were compared with original images Fig.3.(1) to verify this method reasonable. As shown in the figure, the expansion angles of these three numerical values present slight differences, and the bias are between 0.36% and 2.78%. Moreover, the segmentation of flame boundaries in unified standard avoids artificial errors.

Based on the segmentation, brightness and darkness detected edges of binary images were processed and then given digital curves by MATLAB automatically. Sometimes, between upper and lower boundaries there were several little flame vortices shedding, which led to brightness and darkness detected edges of binary images. Therefore, these discrete and mottled circles were removed. The upper and lower boundary were fitted separately by the least square method combined with the optimized FIT method and to assure the corrected fitting curve depicting the original well. And then calculating slope of corrected fitting curve to obtain the angle.

*Corresponding Author: Prof. Fan Yuxin

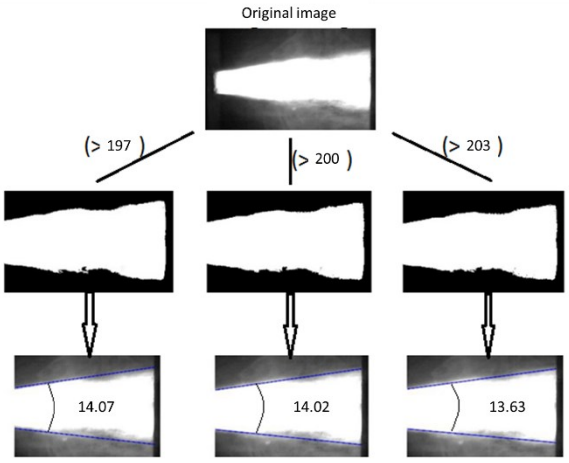

Fig.4 segmentation comparisons at various numerical value ranges

The flame expansion angle fluctuation trends and mean values were shown in Fig.5. The angles of lower and upper boundary were obtained separately by calculating the full angles of the 100 images taken over 0.1s using the method in steps (1)-(6), and then taking the mean value.

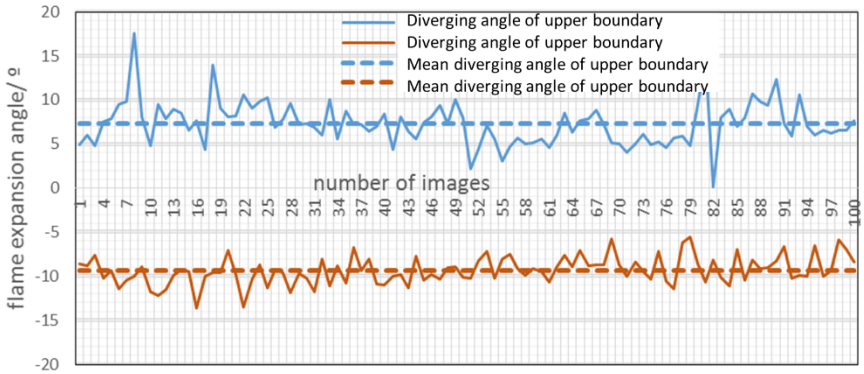

Fig.5 Flame expansion angle fluctuation trends and mean values

2.3 Numerical simulation method

Non-reacting simulation by CFD was performed to analyze the flow characteristics which affected the change of flame expansion angle. The coupling equations of pressure and velocity were solved using the SIMPLE algorithm. A realizable k-e model was chosen as a turbulence model. The near wall region was processed using a non-equilibrium wall functions

*Corresponding Author: Prof. Fan Yuxin

method. The numerical simulation domain is a 2-D rectangular channel of 150mm * 1000mm same with Fig.2.(b), and the distance between the bluff body end edge and the channel exit is 800mm. The refined meshes behind bluff body are structured grids. The detailed boundary conditions are shown in Table 1 [32].

Table 1

Boundary conditions

Boundary conditions	Boundary location	Parameters
Velocity inlet	Inlet	V=50, 100, 150, 200m/s; T=900K
Outflow	Outlet	
Wall	Solid wall and liquid boundary	Stationary wall; no slip; no heat flux

3. Results and Discussion

Flame expansion angle (FEA) is mainly influenced by a number of factors such as blockage ratio (BR), inlet velocity (V) and temperature (T), and equivalence ratio (ϕ). In addition, the blockage ratio is the ratio of frontal/projected/cross-section area (2D area seen from front view) upon the cross-section area of the test section.

$$\text{Blockage Ratio} = \frac{\text{Frontal Area of Model}}{\text{Cross-section area of test section}} \quad \text{Equation 1}$$

And equivalence ratio referred to fuel-air equivalence ratio was defined as the ratio of the fuel-to-oxidizer to the stoichiometric fuel-to-oxidizer ratio. The effect of those factors on the change of FEA will be discussed in detail in this section.

*Corresponding Author: Prof. Fan Yuxin

3.1 Influence of Velocity

The influence of velocity on flame propagation and expansion was with both negative and positive effect. On one side, the growth of axial velocity impaired the propagation into cross flow; on the other side, flow intensity that was accelerated by the growth of velocity enhanced expansion of turbulent flame. To investigate the change of flame expansion, experimental results at 900K were presented in Fig.6. Overall, FEA increased with the growing equivalence ratio, the influence of velocity on FEA differed in various blockage ratios. It was found FEA declined with the increase of velocity at a given blockage ratio (=0.1). Under equivalence ratio =0.7, there was a big difference of FEA between V=100m/s and V=150m/s, but with the increase of equivalence ratio to 0.8, the difference decreased. It demonstrated that when the blockage ratio of stabilizer was of small numerical value, due to incremental effect on chemical reaction rate with the increase equivalence ratio, the inhibition effect of increased velocity on FEA could be weakened.

FEA at a higher blockage ratio (=0.2) first increased and then decreased with the growing velocity with the peak of FEA presented at velocity of 150m/s. Additionally, FEA at velocity=200m/s was bigger than at velocity=100m/s when equivalence ratio was in a range from 0.4 to 0.6. It illustrated that with a bigger blockage ratio, the growth of velocity accelerated FEA in a particular range. Likewise, at blockage ratio = 0.3, FEA first increased and then decreased with the growing velocity, and the peak of FEA appeared at velocity=100m/s was found, also FEA at velocity=200m/s reached the minimum.

In the comparison of the experimental results, the influence of velocity on flame propagation and expansion was related to blockage ratio. Velocity with positive effect on flame expansion achieved the biggest range at blockage ratio = 0.2.

*Corresponding Author: Prof. Fan Yuxin

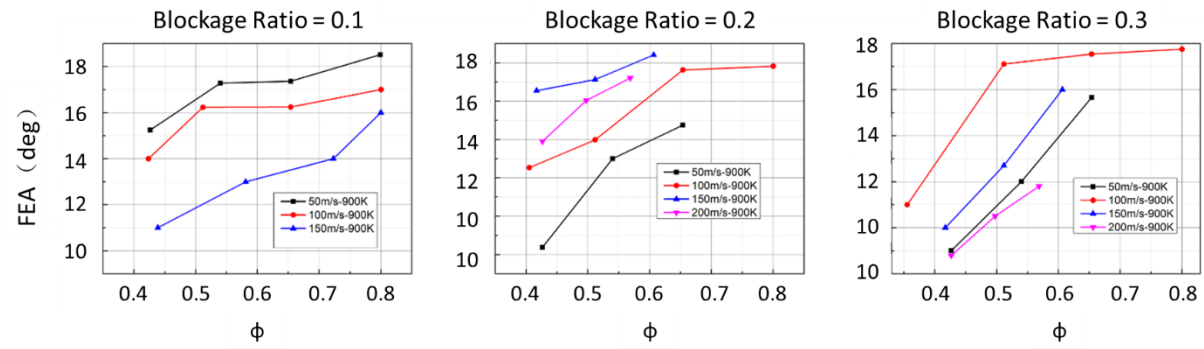

Fig.6 change of FEA at various velocities and blockage ratios

To better investigate the influence of velocity on FEA, relationship between the growth rate of FEA ($(\Delta FEA)_{\%}$) and velocity gradient ($(\Delta V)_{\%}$) was shown at the given equivalence ratio (=0.5) and temperature (=900K) in Fig.7.

Where,

$$(\Delta V)_{\%} = (V - V_0)/V_0 \qquad \text{Equation 1}$$

$$(\Delta FEA)_{\%} = (FEA - FEA_0)/FEA_0 \qquad \text{Equation 2}$$

Setting V_0 = 50m/s, $(FEA)_0$ was the corresponding value to V_0. As demonstrated, $(\Delta FEA)_{\%}$ declined with growth of velocity when blockage ratio was 0.1. However, $(\Delta FEA)_{\%}$ first increased and then decreased with growth of velocity when blockage ratios were 0.2 and 0.3. At blockage ratio = 0.2, there was a relative increase to initial point; however, at blockage ratio = 0.3, there was steep decline after the peak. As analyzed, the influence of velocity on flame expansion was clarified, which was with extreme importance to geometric selection in flame holding system.

*Corresponding Author: Prof. Fan Yuxin

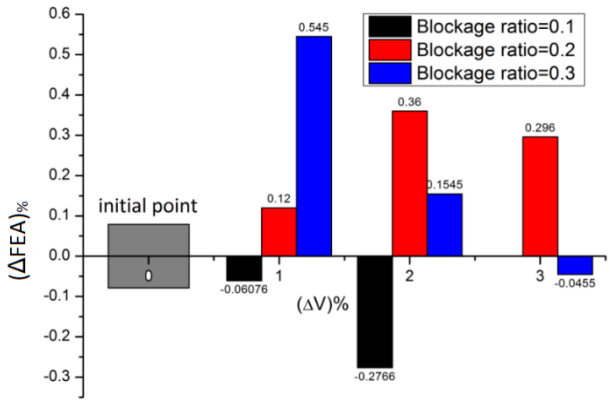

Fig.7 Histogram of FEA growth rates

The influence of velocity on FEA was also reflected in the multidirectional velocity components. The varied ratios of velocity components were related to the flame expansion. 2-D numerical simulations by CFD were carried out to simulate flow, and a schematic of the computational domain was shown in Fig.8. Moreover, velocity components ratio, namely V(x)/V, was defined in CFD-post. V(x)/V data curves located at 10mm in the rear of V-gutter were compared with various velocities. The bigger numerical value of V(x)/V indicated a greater mixing ability of vortex and surroundings, and that was well suited to flame spreading perpendicular to axial flow. Fig.8 showed V(x)/V data curves at various blockage ratios (e.g. 0.1, 0.2, and 0.3). It was found that V(x)/V declined with the increase of velocity when blockage ratio was 0.1. Whereas V(x)/V first increased and then decreased with the increasing velocity; the peak of V(x)/V presented at a certain velocity (=150m/s) as blockage ratio was 0.2 and the other certain velocity (100m/s) as blockage ratio was 0.3. Thus, the influence of V(x)/V played an auxo-action on flame spreading. Also, the change of V(x)/V was corresponding to change of FEA and $(\Delta FEA)_{\%}$.

*Corresponding Author: Prof. Fan Yuxin

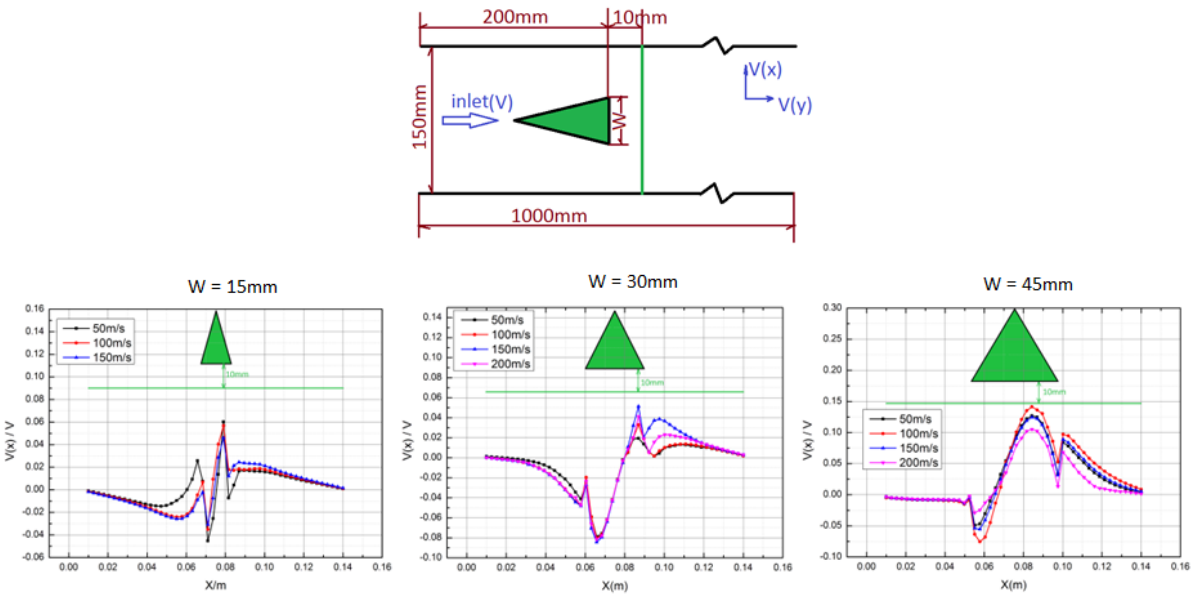

Fig.8 V(x)/V data curves located 10mm downstream of stabilizers at different blockage ratios

3.2 FEA related with Temperature

The influence of temperature on FEA was related to chemical reaction rate directly. As temperature grew, activation energy was reduced. Fig. 9 showed the experimental results, FEA increased first and then decreased with growing temperature; and the peak of FEA appeared at 750K. Chemical characteristics of Kerosene/air premixed combustible had changed at high temperature. A mixture of *n*-decane and 1,2,4-trimethybenzene (8 : 2, by weight), called the Aachen surrogate, was selected for consideration as a possible surrogate of kerosene [33]. Side reactions occurred to *n*-decane above 900K, which led to a converse effect on flame spreading [34]. Moreover, when the blockage ratio was 0.2, equivalence ratio had an obvious effect on FEA at a lower temperature of 450K, due to the sudden increase at equivalence ratio from 0.6 to 0.7. Also, at blockage ratio = 0.3, there were obvious increases with equivalence ratio when temperatures were 450K and 600K. However, it presented a

*Corresponding Author: Prof. Fan Yuxin

small increase with growing equivalence ratio at 900K, which was different from the others.

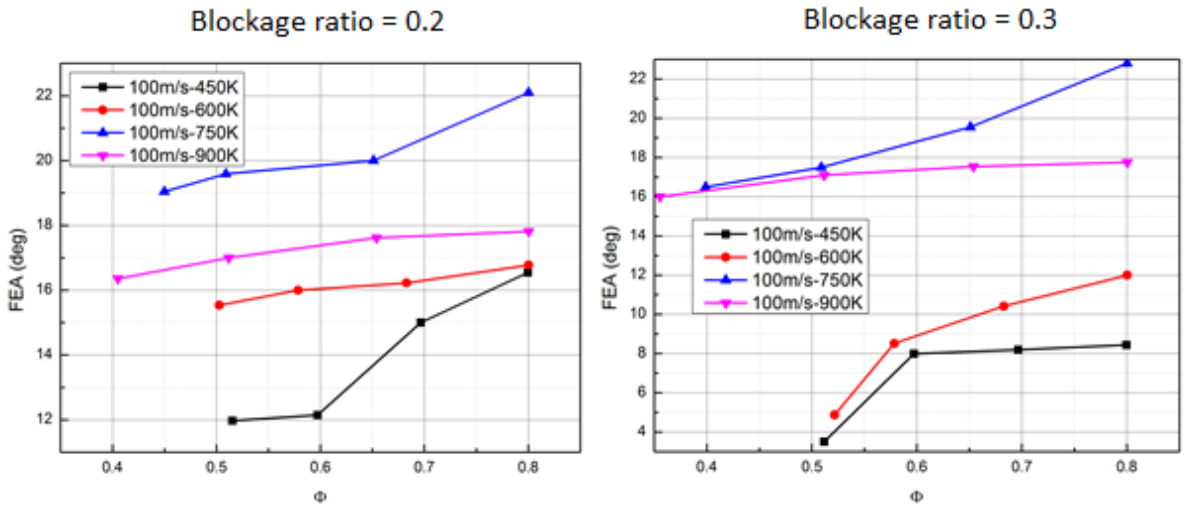

Fig.9 Line graphs of FEA at different temperatures

3.3 FEA related with Blockage Ratio

Blockage ratio was a key issue for stabilizer design, because of its flame stabilization and flow resistance. Fig. 10 presented the processed results to investigate the change of FEA with blockage ratio. As shown, FEA at 900K was almost the same with blockage ratio 0.2 and 0.3, and both of them were bigger than it with blockage ratio 0.1; however, FEA with blockage ratio 0.2 was much bigger than it with blockage ratio 0.3 at 450K. Therefore, it demonstrated a stabilizer with blockage ratio 0.2 could increase FEA and reduce flow resistance.

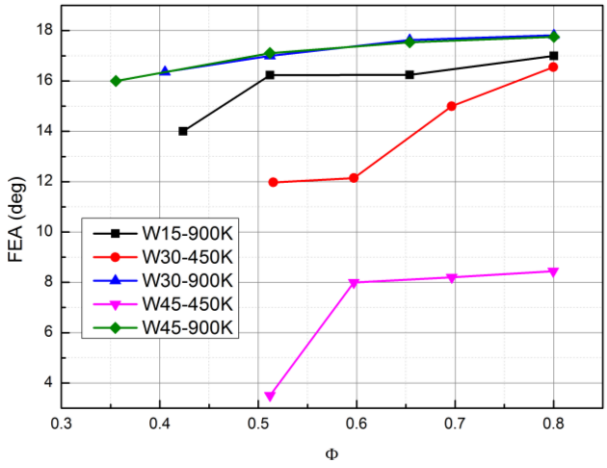

Fig.11 change of FEA at different blockage ratios

*Corresponding Author: Prof. Fan Yuxin

4. Conclusions

The change of FEA with blockage ratio, equivalence ratio, velocity, and temperature was investigated in this work. Flame images taken by a high-speed camera were processed by programs MATLAB. The following conclusions were drawn:

(1) Through the steps of segmentation, detection, removal, separation, and fitting done by programming, the image processing had the features of high precision and efficiency, reduced the artificial errors, as well as created a good method to obtain flame boundary.

(2) There was an incremental impact of fuel/air equivalence ratio on FEA in lean premixed combustion. Velocity and temperature were two main aerodynamic parameters related to FEA, which did not increase or decrease monotonically but had a peak value. The change of FEA with temperature and velocity had its significance for design and layout of stabilizers.

(3) Blockage ratio was another key parameter for FEA, which was related to not only flame stabilization also flow resistance. In order to avoid extra total pressure loss and insure combustion stability, it was necessary to select appropriate blockage ratio according to the change of FEA. As presented, BR0.2 was the best for increasing FEA and reducing total pressure loss.

*Corresponding Author: Prof. Fan Yuxin

References

[1] Ellis, O. D. C. (1928). Flame movement in gaseous explosive mixtures. J. Fuel Sci., 7, 502-508.
[2] Markstein, G. H. (Ed.). (2014). Nonsteady flame propagation: AGARDograph (Vol. 75). Elsevier.
[3] Hassanvand, A., Gerdroodbary, M. B., Fallah, K., & Moradi, R. (2018). Effect of dual micro fuel jets on mixing performance of hydrogen in cavity flameholder at supersonic flow. International Journal of Hydrogen Energy, 43(20), 9829-9837.
[4] Ma H K, Harn J S. The jet mixing effect on reaction flow in a bluff-body burner[J]. International journal of heat and mass transfer, 1994, 37(18): 2957-2967.

[5] Sazhin, S. S., Abdelghaffar, W. A., Sazhina, E. M., & Heikal, M. R. (2005). Models for droplet transient heating: effects on droplet evaporation, ignition, and break-up. International journal of thermal sciences, 44(7), 610-622.

[6] Souflas, K., & Koutmos, P. (2018). On the non-reacting flow and mixing fields of an axisymmetric disk stabilizer, under inlet mixture stratification and preheat. Experimental Thermal and Fluid Science, 99, 357-366.

[7] Schneider, G. M., Nathan, G. J., & O'Doherty, T. (2004). Implications on flame stabilization in a precessing jet flame from near field velocity measurements. Proceedings of the Institution of Mechanical Engineers, Part A: Journal of Power and Energy, 218(8), 677–687.

[8] Dellimore K H. Investigation of Fuel-air Mixing in a Micro-flameholder for Micro-power and Scramjet Applications[D]. , 2005.

[9] Xiouris, C., & Koutmos, P. (2011). An experimental investigation of the interaction of swirl flow with partially premixed disk stabilized propane flames. Experimental Thermal and Fluid Science, 35(6), 1055-1066.

[10] Fu, W., Li, F., Zhang, H., Yi, B., Liu, Y., & Lin, Q. (2019). Liftoff behaviors and flame structure of dimethyl ether jet flame in CH4/air vitiated coflow. Proceedings of the Institution of Mechanical Engineers, Part A: Journal of Power and Energy.

[11] Zhao, S., & Fan, Y. (2019). Experimental and numerical study on thermodynamic performance in a designate pilot-ignition structure: Step. Aerospace Science and Technology, 91, 561-570.

[12] Greenhalgh, D. A. (2000). Laser imaging of fuel injection systems and combustors. Proceedings of the Institution of Mechanical Engineers, Part A: Journal of Power and Energy, 214(4), 367–376.

[13] Chowdhury, B. R., & Cetegen, B. M. (2017). Experimental study of the effects of free stream turbulence on characteristics and flame structure of bluff-body stabilized conical lean premixed flames. Combustion and Flame, 178, 311-328.

*Corresponding Author: Prof. Fan Yuxin

[14] Hashemi, S. M., & Hashemi, S. A. (2019). Investigation of the premixed methane–air combustion through the combined porous-free flame burner by numerical simulation. Proceedings of the Institution of Mechanical Engineers, Part A: Journal of Power and Energy.

[15] Alviso, D., Mendieta, M., Molina, J., & Rolón, J. C. (2017). Flame imaging reconstruction method using high resolution spectral data of OH*, CH* and C2* radicals. International Journal of Thermal Sciences, 121, 228-236.

[16] Brequigny, P., Endouard, C., Mounaïm-Rousselle, C., & Foucher, F. (2018). An experimental study on turbulent premixed expanding flames using simultaneously Schlieren and tomography techniques. Experimental Thermal and Fluid Science, 95, 11-17.

[17] Kamal, M. M., & Amohamad, A. (2007). Investigation of liquid fuel combustion in a cross-flow burner. Proceedings of the Institution of Mechanical Engineers, Part A: Journal of Power and Energy, 221(3), 371–385.

[18] Hashemi, S. M., & Hashemi, S. A. (2019). Numerical study of the flame stability of premixed methane–air combustion in a combined porous-free flame burner. Proceedings of the Institution of Mechanical Engineers, Part A: Journal of Power and Energy, 233(4), 530–544.

[19] Gong, F., Huang, Y., & Huang, X. (2015). Size effect on the flame base locations after V-gutters for premixed flames. International Journal of Heat and Mass Transfer, 82, 406-418.

[20] Rochette, B., Collin-Bastiani, F., Gicquel, L., Vermorel, O., Veynante, D., & Poinsot, T. (2018). Influence of chemical schemes, numerical method and dynamic turbulent combustion modeling on LES of premixed turbulent flames. Combustion and Flame, 191, 417-430.

[21] Zettervall, N., Nordin-Bates, K., Nilsson, E. J. K., & Fureby, C. (2017). Large Eddy Simulation of a premixed bluff body stabilized flame using global and skeletal reaction mechanisms. Combustion and Flame, 179, 1-22.

[22] Zhou, B., Sobiesiak, A., & Quan, P. (2006). Flame behavior and flame-induced flow in a closed rectangular duct with a 90 bend. International Journal of Thermal Sciences, 45(5), 457-474.

[23] Umyshev, D. R., Dostiyarov, A. M., Tumanov, M. Y., & Qiuwang, W. A. N. G. (2017). EXPERIMENTAL INVESTIGATION OF V-GUTTER FLAMEHOLDERS. Thermal Science, 21(2).

[24] Lubarsky E, Cross C, Fricker A, et al. Dynamics of V-gutter-stabilized Jet-A Flames in a Single Flame Holder Combustor with Full Optical Accesss[C]//45th AIAA/ASME/SAE/ASEE Joint Propulsion Conference & Exhibit. 5291.

[25] Alemi, E., & Zargarabadi, M. R. (2017). Effects of jet characteristics on NO formation in a jet-stabilized combustor. International Journal of Thermal Sciences, 112, 55-67.

*Corresponding Author: Prof. Fan Yuxin

[26] Elkotb, M. M., & Shehata, M. S. (2003). Effect of flame stabilizer geometry on emissions of turbulent premixed blended flames. Experimental thermal and fluid science, 27(4), 343-353.

[27] Lipardi, A. C., Bergthorson, J. M., & Bourque, G. (2016). NOx emissions modeling and uncertainty from exhaust-gas-diluted flames. Journal of Engineering for Gas Turbines and Power, 138(5), 051506.

[28] Driscoll, J. F. (2008). Turbulent premixed combustion: Flamelet structure and its effect on turbulent burning velocities. Progress in energy and Combustion Science, 34(1), 91-134.

[29] Clavin, P. (1985). Dynamic behavior of premixed flame fronts in laminar and turbulent flows. Progress in energy and combustion science, 11(1), 1-59.

[30] Lipatnikov, A. N., & Chomiak, J. (2002). Turbulent flame speed and thickness: phenomenology, evaluation, and application in multi-dimensional simulations. Progress in energy and combustion science, 28(1), 1-74.

[31] Salzano, E., Marra, F. S., Russo, G., & Lee, J. H. S. (2002). Numerical simulation of turbulent gas flames in tubes. Journal of Hazardous Materials, 95(3), 233-247.

[32] Zhao, S., & Fan, Y. (2019). Experimental and numerical study on thermodynamic performance in a designate pilot-ignition structure: Step. Aerospace Science and Technology, 91, 561-570.

[33] Honnet, S., Seshadri, K., Niemann, U., & Peters, N. (2009). A surrogate fuel for kerosene. Proceedings of the Combustion Institute, 32(1), 485-492.

[34] Zeng, M., Yuan, W., Wang, Y., Zhou, W., Zhang, L., Qi, F., & Li, Y. (2014). Experimental and kinetic modeling study of pyrolysis and oxidation of n-decane. Combustion and Flame, 161(7), 1701-1715.

*Corresponding Author: Prof. Fan Yuxin